Contents lists available at ScienceDirect

Journal of Affective Disorders

journal homepage: www.elsevier.com/locate/jad

Research paper

Functional network topology associated with apathy in Alzheimer's disease

Shankar Tumati[a,*], Jan-Bernard C. Marsman[a], Peter Paul De Deyn[b,c], Sander Martens[a], André Aleman[a,d,^], for the Alzheimer's Disease Neuroimaging Initative

[a] NeuroImaging Center, University of Groningen, University Medical Center Groningen, the Netherlands
[b] Department of Neurology, University of Groningen, University Medical Center Groningen, the Netherlands
[c] Laboratory of Neurochemistry and Behaviour, Institute Born-Bunge, University of Antwerp, Belgium
[d] Department of Psychology, University of Groningen, the Netherlands

ARTICLE INFO

ABSTRACT

Background: Apathy, a common neuropsychiatric (NPS) in patients with mild cognitive impairment (MCI) and Alzheimer's disease (AD), is associated with structural and metabolic brain changes. However, functional connectivity changes across the brain in association with apathy remain unclear. In this study, graph theoretical measures of integration and segregation from resting state functional connectivity in MCI and AD patients with low depression scores, and healthy controls.

Methods: In MCI and AD patients with low depression scores, graph theoretical measures of integration and segregation were derived from resting state functional connectivity in patients, which were compared between those with apathy (NPS_A, $n = 21$) to those without NPS (NPS_None, $n = 28$) and those with NPS other than apathy (NPS_NA, $n = 38$). Additionally, the same measures were compared between AD patients and healthy controls (amyloid uptake below threshold levels).

Results: Altered whole brain global efficiency and reduced local efficiency were found in NPS_A compared to NPS_None and NPS_NA. In similar contrasts, apathy was associated with increased participation coefficient in the frontoparietal and cingulo-opercular template-based networks. A study-specific network definition also showed similar results. In comparison, AD patients showed higher modularity compared to controls at the whole brain level and higher participation coefficient in the ventral attention network.

Limitations: The severity and dimensions of apathy were not assessed.

Conclusions: Loss of segregation in the frontoparietal and cingulo-opercular network, which are involved in the control of goal-directed behavior, was associated with apathy in MCI/AD. The results also suggest that network-level changes in AD patients may underlie specific NPS.

CDR	clinical dementia rating scale
CON	cingulo-opercular network
dACC	dorsal anterior cingulate cortex
FPN	frontoparietal network
Ins-TPN	insulo-temporoparietal network
NPI	Neuropsychiatric inventory
NPS	Neuropsychiatric symptoms
NPS_A	Neuropsychiatric symptoms with apathy
NPS_NA	Neuropsychiatric symptoms other than apathy
NPS_None	Neuropsychiatric symptoms absent
rs-fMRI	resting state functional magnetic resonance imaging

SN	salience network

1. Introduction

Apathy, characterized by a lack of interest in routine and new activities, and a flat emotional affect, (Robert et al., 2009) is a common neuropsychiatric symptoms (NPS) associated with poor functional outcomes in Alzheimer's disease (AD) (Geda et al., 2008; Onyike et al., 2007; Spalletta et al., 2010). These symptoms are thought to result from disrupted fronto-subcortical circuits that underlie motivation and its transformation to action (Nobis and Husain, 2018; Starkstein and

Brockman, 2018). Although structural and metabolic changes in the dorsal anterior cingulate cortex, prefrontal cortex, basal ganglia, superior and inferior temporal lobe, and lateral parietal lobe have been associated with apathy, (Kos et al., 2016; Moretti et al., 2017; Stella et al., 2014; Theleritis et al., 2014; Tumati et al., 2018) corresponding changes in functional connectivity are understudied.

Graph theoretical analysis enables quantification of network structure of functional connections derived from resting state functional imaging of the brain, which shows an optimum network structure (Bullmore and Sporns, 2009). In AD, the segregated processing of information, measured using the modularity metric, (Brier et al., 2014; Pereira et al., 2016) as well as the integration of information from different modules or networks, measured with the path length metric, are found to be increased (Dai et al., 2015; Deng et al., 2016; Filippi et al., 2018; Liu et al., 2014). With respect to apathy in AD, studies of functional networks are limited to analyses of selective large-scale functional networks where a role for the frontoparietal network is suggested (Joo et al., 2017; Munro et al., 2015). However, not all studies support this finding, (Balthazar et al., 2014) and to our knowledge, topological changes associated with apathy have not been described. Based on the literature, we hypothesized that graph theoretical measures of functional sub-networks such as the FPN and the salience network would be altered in apathy. Further, these localized changes in individual networks would result in altered graph theoretical measures at the global level.

2. Materials and methods

Data used in this study were obtained from the Alzheimer's Disease Neuroimaging Initiative (ADNI) database (http://adni.loni.usc.edu). ADNI was launched in 2003 as a public-private partnership, led by Principal Investigator Michael W. Weiner, MD. The primary goal of ADNI has been to test whether serial magnetic resonance imaging (MRI), positron emission tomography (PET), other biological markers, and clinical and neuropsychological assessment can be combined to measure the progression of mild cognitive impairment (MCI) and early Alzheimer's disease (AD). Further information on subject recruitment for this study can be found at http://www.adni-info.org. Institutional review boards at each site approved the study. Written informed consent was obtained from all subjects and study partners. Notably, only those scoring less than 6 on the 15-item Geriatric Depression scale were included. All study procedures are described in detail on the study website (http://adni.loni.usc.edu/methods/documents/, *ADNI 2 Procedures Manual*).

2.1. Subjects

In the present study, subjects with a baseline rs-fMRI scan from the ADNI2 cohort were included. The analysis consisted of two parts. We first assessed differences in graph metrics (detailed below) between AD subjects ($n = 26$) and healthy controls (HC, $n = 18$), who were defined as cognitively normal (according to ADNI inclusion criteria) and with cortical amyloid tracer (AV-45) retention below 1.11 standardized uptake value ratio (SUVR) (Landau et al., 2012). This comparison provides a context to changes associated with apathy. Next, in a broader sample ($n = 87$) of MCI as well as AD subjects, three sub-groups were defined – those with i) apathy (NPS_A, $n = 21$), ii) without NPS (NPS_None, $n = 28$), and iii) NPS other than apathy (NPS_NA, $n = 38$). NPS were assessed with the Neuropsychiatric Inventory (NPI, described below). The ADNI study specify permitted and excluded medications, details of which are described in the document linked in Sec. 2. Subjects were required to be on stable dosage of permitted medications for 4 weeks prior to the intake screening. These data were retrieved from the ADNI database for subjects in the current study and shown in SI Table 2.

2.2. Assessments

At baseline, all subjects underwent neuropsychological tests including the Mini Mental State Examination (MMSE), Clinical Dementia Rating (CDR) assessment, and the 13-item Alzheimer's Disease Assessment Scale (ADAS). The NPI is a validated and reliable instrument assessing twelve NPS (Cummings et al., 1994). It is administered to the study partner (known to the subject or preferably living with him/her) in the absence of the subject and assesses the presence or recent development of NPS in the preceding four weeks. To assess apathy, study partners were asked the following: 'Has the patient lost interest in the world around him/her? Has he/she lost interest in doing things or does he/she lack motivation for starting new activities? Is he/she more difficult to engage in conversation or in doing chores? Is the patient apathetic or indifferent?' Subjects in this study were considered apathetic if the study partner answered 'yes' in response to the above questions. The present study utilized the diagnosis of apathy, and not the severity of apathy symptoms. The NPI Apathy total score (severity: 3-point scale, & distress: 5-point scale) was 4.19 (2.6) (AD: 3.9 (2.64), MCI: 4.45 (2.66)). No apathy-specific scales were available in the database. Other NPS were similarly assessed with symptom-specific questions. The NPS_None group was defined by a total NPI score of zero; the NPS_NA group was defined by a total NPI score greater than zero and a NPI-apathy score of zero. In addition to the NPI, the study partner was administered the Functional Assessment Questionnaire (FAQ) (Pfeffer et al., 1982).

2.3. Image acquisition and processing

Subjects were scanned on 3.0 Tesla Philips MRI scanners at thirteen sites. Echo-planar images with repetition time/echo time (TR/TE) of 3000/30 ms and flip angle (FA) of 80° were acquired in an interleaved manner. Each scan consisted of 140 vol, with 48 slices, dimensions 64 × 64 and voxel size 3.31 × 3.31 × 3.31 mm. Structural images with a resolution of 1 × 1 × 1.2 mm were acquired through the sagittal plane, using a magnetization prepared rapid gradient echo (MPRAGE) three-dimensional T1-weighted sequence with a TR = 6.8 ms, TE = 3.16 ms, and FA = 9°. Scans were acquired a maximum of 81 days prior to NPI assessment (mean (SD) = 18.6 (15.0) days).

The resting state scan lasting seven minutes was acquired with subjects asked to keep their eyes closed. An overview of the processing steps are provided in Fig. 1. These consisted of (i) discarding the first three volumes of the scan to achieve signal equilibrium; (ii) correction for slice timing and intensity differences due to interleaved acquisition; (iii) spatial realignment to the first volume using rigid body transformation to correct for head motion, and coregistration to the subject's high resolution structural scan; (iv) intensity scaling to a mode value of 1000 (performed using *fslmath* in the FSL suite), and (v) normalization to a study specific anatomical template created using DARTEL (Diffeomorphic Anatomical Registration through Exponentiated Lie Algebra toolbox) and resampled to 3 mm isotropic voxels. Finally, data were demeaned and detrended (linear) and the following parameters were regressed out – (1) the global signal, (2) white matter, (3) cerebrospinal fluid signal and (4) motion parameters from the realignment step, and their first order derivatives. We chose to perform global signal regression as it was shown to strongly reduce motion related artifacts when combined with censoring of motion affected volumes and reduces the need to censor volumes subsequent to the movement affected volume (Power et al., 2014). Next, temporal band pass filtering using an eighth order Butterworth filter with zero phase was performed to retain frequencies in the range of 0.009 to 0.08 Hz. Finally, data were spatially smoothed with a 6 mm FWHM (full width half maximum) kernel.

Minimizing motion artifacts: To minimize motion-induced spurious correlations (Power et al., 2014; Van Dijk et al., 2012), scans were examined for excessive motion defined by framewise displacement (FD) and standardized delta variations in signal intensity (DVARS). FD
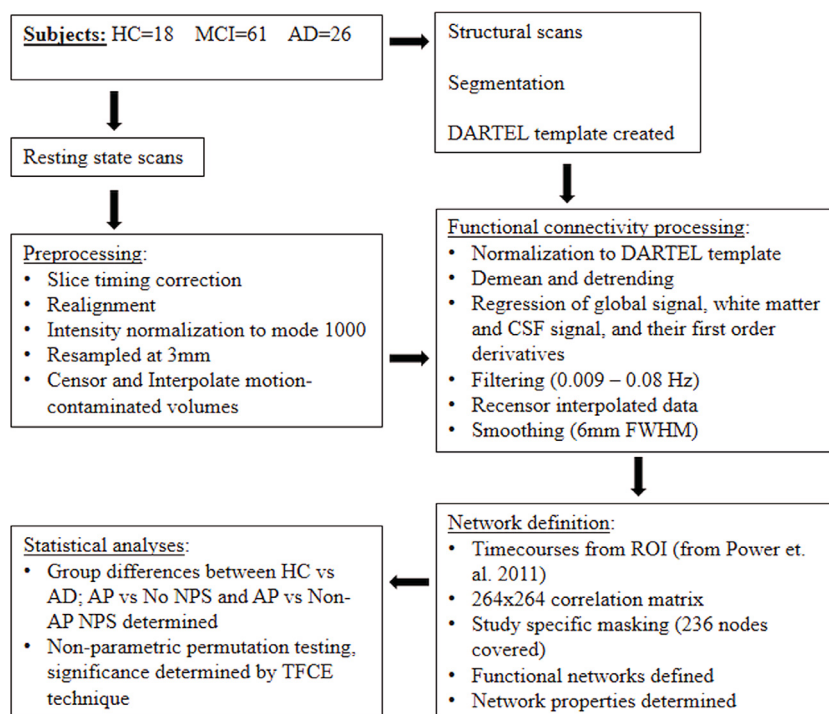
Fig. 1. Overview of processing steps.

estimates head motion from one volume to next and is calculated as the sum of the absolute displacement in translational and rotational motion. Rotational measures were transformed to millimeters by assuming that the center of rotation was located 65 mm away from the affected voxels. The DVARS measure determines changes in signal intensity from one volume to the next and is calculated at the global level as the root mean square of the temporal derivative of the time series at each voxel. Volumes where FD exceeded 0.5 mm and DVARS exceeded 3 standard deviations (with first volume set at zero) were censored. If less than five minutes of valid volumes (100 vol, 73% of the scan) remained after censoring then those scans were excluded from further analysis ($n = 8$). For remaining scans, censored volumes were replaced by spline interpolation, and were re-censored after frequency filtering. On average, 5.08% volumes in each scan were censored (AD = 4.2%, MCI = 4.29%, HC = 6.9%). These steps were performed prior to regression of spurious signals and filtering. The interpolated scans were re-censored prior to determining functional connectivity.

Connectivity matrices: The mean time course of activity was extracted from 264 ROIs (Power et al., 2011). Any ROI with <50% coverage in any subject was excluded (28 ROIs). The Pearson's correlation coefficient between the time courses of each pair of ROI was calculated, resulting in 236 × 236 connectivity matrix. Further details for calculating connectivity matrices, graph theoretical measures and network definition are given in SI Methods.

2.4. Network definition

Based on the modularity metric, seven functional networks were defined in the current sample (SI Fig. 1A, method described in SI Method). These were labeled as – visual network (VS, 52 nodes), somato-motor network (SMN, 43 nodes), insulo-temporoparietal network (Ins-TPN, 39 nodes), FPN (24 nodes), DMN (64 nodes), dorsal anterior cingulate network (dACC, 6 nodes), and subcortical network (8 nodes). Network assignment of each node for both network definitions are given in SI Table 1. In addition, a standard network definition from independent young healthy subjects was used (SI Fig. 1B, SI Methods & SI Table 1) (Power et al., 2011). Both network definitions were used as

the disease process may alter healthy network structures but definitions may also be influenced by the parcellation method.

We assessed global efficiency where higher values reflect a more integrated network. Measures of segregation were determined at the nodal level with local efficiency, and for groups of nodes with clustering coefficient. Higher values for both measures of segregated neural processing indicate higher local density of edges. Segregation was also assessed globally by modularity where higher values indicate increased segregation. For each functional network in both definitions, mean local efficiency representing intra-network density of edges and mean participation coefficient where higher values indicate lower edges within the network or higher inter-network edges (Rubinov and Sporns, 2010).

2.5. Statistical analysis

Graph measures were determined over a range of network densities by retaining 1% to 30% (in steps of 1%) of the strongest correlations in the connectivity matrices. Differences in graph measures between (i) HC and AD, (ii) NPS_None and NPS_A, and (iii) NPS_NA and NPS_A were determined after controlling for age and gender. Significance of the differences in network measures was non-parametrically tested by randomly permuting group membership 5000 times for each comparison (maintaining group sizes). A null distribution of group differences for each comparison was computed at each threshold and tested for significance, considered at $p < .05$ (two-sided), using threshold free cluster enhancement (TFCE) (with default settings-$E = 0$, $H = 1$) (Smith and Nichols, 2009).

All analyses were conducted in MATLAB 2014a (The MathWorks, Inc., Natick, USA), unless noted otherwise, using custom in-house scripts. Preprocessing steps (except intensity normalization) were performed in SPM12b (http://www.fil.ion.ucl.ac.uk/spm/software/spm12). SI Fig. 1 was created using BrainNet Viewer (http://www.nitrc.org/projects/bnv/).

Table. 1

Sample characteristics of healthy control and AD, and MCI and AD subjects without any NPS (NPS_None), with NPS other than apathy (NPS_NA), and apathy (NPS_A).

	HC	AD	NPS_None	NPS_NA	NPS_A	$\chi^{2\$}$	p
n (female)	18 (11)	26 (12)	28 (12)	38 (21)	21 (5)	5.39	.07
n (AD)	–	–	4	12	10	6.38	.04
Age	73.13 (5.7)	72.87 (7.2)	71.22 (6.3)	71.29 (7.6)	75.27 (5.7)	5.18	.07
Education	16.56 (1.8)	15.88 (2.7)	16.18 (2.5)	16.16 (2.7)	15.76 (2.6)	0.41	.81
MMSE	28.61 (1.5)	22.35 (2.5)	26.75 (3.0)	26.05 (3.2)	25.48 (3.4)	2.38	.30
ADAS-13	9.28 (3.9)	35.58 (9.2)	19.71 (11.4)	20.08 (11.4)	25.57 (12.5)	4.01	.13
CDR-SB	0.03 (0.1)	4.40 (1.4)	1.64 (1.5)	2.49 (1.6)	3.57 (1.6)	18.62	<.01
FAQ	0.11 (0.5)	15.00 (7.8)	3.70 (6.9)	7.26 (7.9)	12.19 (6.0)	22.12	<.01
Total NPI	0.61 (1.0)	9.23 (11.3)	–	5.13 (5.2)	12.81 (11.1)	10.76	<.01[#]
Hippocampal volume (bilateral, mm³)	7029.2 (783.8)	6068.7 (1050.0) (n = 23)	7085.7 (1070.6) (n = 23)	6837.20 (1369.6) (n = 36)	6637.41 (933.0) (n = 19)	1.05	.59
Amyloid uptake (AV45)	1.02 (0.04)	1.47 (0.2) (n = 25)	1.22 (0.2)	1.31 (0.2) (n = 37)	1.39 (0.3)	6.21	.04
FDG-PET	6.79 (0.4)	5.24 (0.7)	6.17 (0.9)	6.02 (0.7)	5.64 (0.6)	8.37	.02

[$] χ^2 statistic for Kruskal-Wallis test (two-tailed)

[#] comparison between NPS_NA and NPS_A groups; AV45: Amyloid binding ligand, values in Standardized Uptake Value Ratio (SUVR); FDG-PET: Glucose metabolism, values in SUVR; ADAS-13: Alzheimer's Disease Assessment Scale-13 item; FAQ: Functional Assessment Questionnaire; CDR-SB: Clinical Dementia Rating scale-sum of boxes; NPI: Neuropsychiatric Inventory score

3. Results

3.1. Sample characteristics

Table 1 presents demographic, neuropsychological and neuropsychiatric assessments, and imaging characteristics of HC and AD, and MCI and AD subjects with NPS_None, NPS_NA, and NPS_A groups. The NPS_A group showed a worse neuropsychological and AD-related biomarker profile compared to NPS_None and NPS_NA groups. The NPS_A group had significantly higher CDR scores, reduced functional abilities and a higher total neuropsychiatric burden along with higher cerebral amyloid deposition and lower cerebral glucose metabolism.

3.2. Whole brain topological properties

In the AD group, modularity was significantly higher compared to HC in binary (1–20% network density) and weighted graphs (1–30% network density) (Fig. 2). No significant differences were found between HC and AD in other global graph metrics. Subjects with apathy showed lower local efficiency compared to NPS_None and NPS_NA groups in binary (8–24% & 9–30% network density, respectively) and weighted graphs (5–30% & 1–30% network density, respectively). Global efficiency also differed between the groups. However, compared to the NPS_None and NPS_NA groups, global efficiency was lower in the NPS_A group in weighted graphs (10–30% & 9–30% network density, respectively), but higher in binary graphs (5–30% & 2–30% network density, respectively). Clustering coefficient was reduced in the NPS_A group as compared to the NPS_NA group in binary (5–30% network density) and weighted (1–30% network density) graphs. The NPS_A group also showed lower modularity compared to the NPS_NA group but only over a narrow range of network densities in binary graphs (11–13 and 16–22%).

3.3. Group differences in functional brain networks

In study-specific networks (Fig. 3), compared to the HC group, the AD group showed significantly reduced local efficiency in the dACC network in binary and weighted graphs (4–28% and 5–30% network density, respectively) and higher participation coefficient in the Ins-TPN (binary: 3–30%, weighted: 4–30%). No further differences were found between HC and AD in other networks. Participation coefficient in the NPS_A group was higher in the FPN compared to the NPS_NA group (binary: 3–30%, weighted: 3–30%) and in the dACC network compared to the NPS_None group (binary: 20, 27–30%, weighted: 8–30%) and the NPS_NA group (binary: 3–30%, weighted: 3–30%). The

NPS_None group also showed higher local efficiency in the subcortical network (binary: 3–30%, weighted: 3–30%) (SI Fig. 2) and lower participation coefficient in the somatomotor network (binary: 3–30%, weighted: 4–30%) compared to the NPS_A group (SI Fig. 3). Participation coefficient in the subcortical network was lower in the NPS_NA group compared to NPS_A group (binary: 2–24%, weighted: 2–29%) (SI Fig. 3).

In network definitions by Power et al. (2011) (Fig. 4), participation coefficient was higher in the ventral attention network in AD compared to HC (binary: 4–30%, weighted: 7–30%). No other significant differences were found between HC and AD in any network. Compared to the NPS_None and NPS_NA group, the NPS_A group showed higher participation coefficient in the FPN (binary: 5–30%, weighted: 5–30% & binary: 2–30%, weighted: 2–30%, respectively), cingulo-opercular network (CON) (binary: 5–30%, weighted: 6–30% & binary: 7–30%, weighted: 7–30%, respectively), and salience network (binary: 8–30%, weighted: 8–30% & binary: 13–17, 19–20%, weighted: 13–16, 19%, respectively). The NPS_A group showed higher local efficiency than the NPS_NA group in the DAN (binary: 1–30%, weighted: 1–30%) (SI Fig. 4). Further, the NPS_None group showed higher local efficiency in the subcortical network (binary: 20–27%, weighted: 16–30%) (SI Figure 5) and lower participation coefficient in the somatomotor network (binary: 3–30%, weighted: 3–30%) than in the NPS_A group (SI Figure 6). Finally, the NPS_NA group showed higher local efficiency (binary: 11–25%, weighted: 4–30%) (SI Fig. 4) and lower participation coefficient (binary: 8–10%, weighted: 6–29%) (SI Figure 6) in the DMN as compared to the NPS_A group.

We also considered whether graph theoretical measures differed between AD with apathy (n = 10) and MCI with apathy (n = 11). The AD apathy group showed lower global efficiency, and lower local efficiency in the DMN and salience network than in the MCI apathy group. Given the small sample size, the results are exploratory in nature and are described in the supplementary results.

4. Discussion

This study aimed to determine the topological properties of functional brain networks associated with apathy in MCI and AD. Subjects with apathy were more likely to have AD, have higher scores on the CDR (sum of boxes), NPI and FAQ, higher global amyloid deposition, and lower cortical glucose metabolism compared to those without any NPS and those with NPS other than apathy. The topological measures in the AD group showed increased modularity as compared to the HC group while global efficiency, local efficiency, and clustering coefficient did not differ. In AD/MCI patients with apathy, global mean local
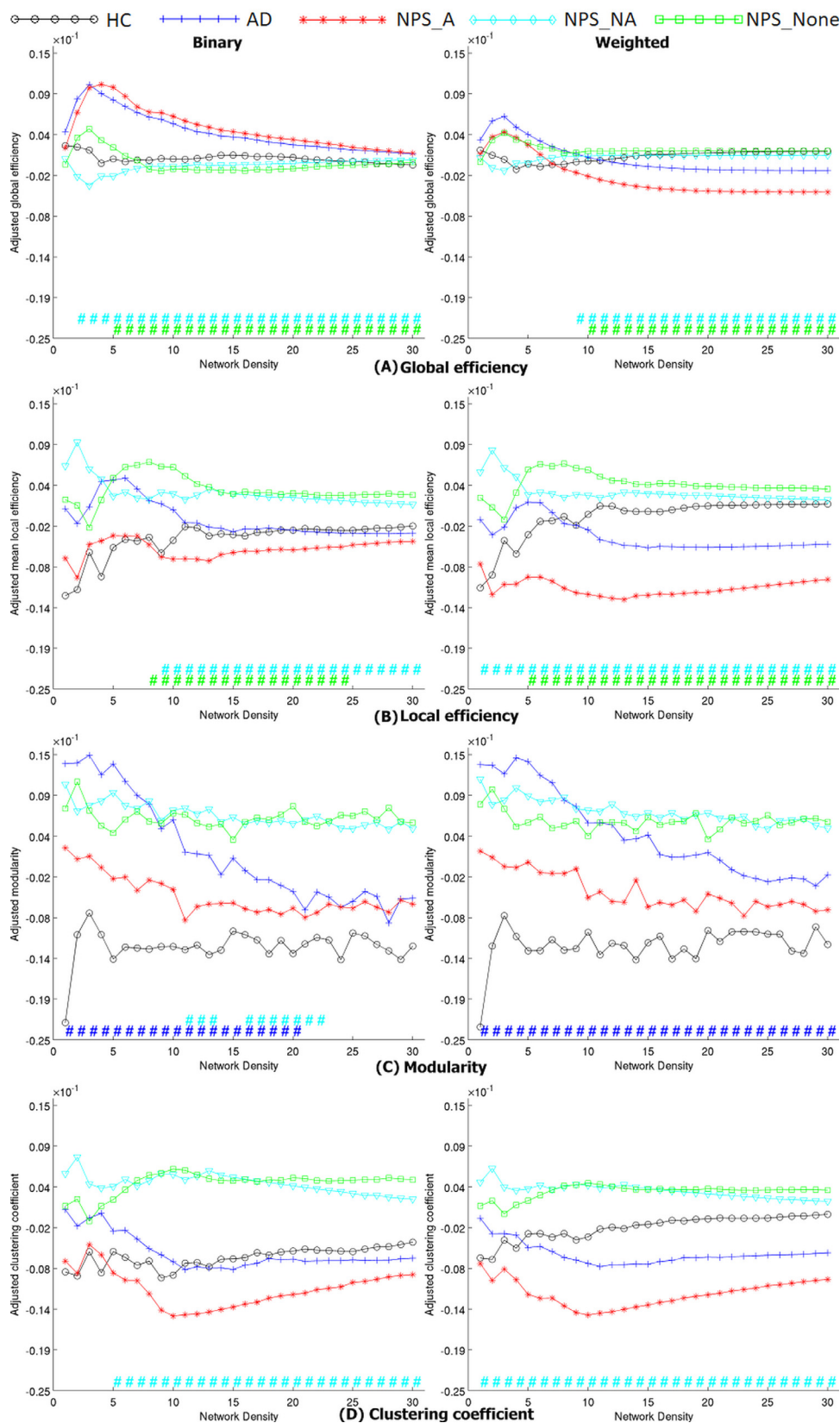
Fig. 2. Whole brain graph theoretical measures. The figures show the binary (left) and weighted (right) global efficiency (A), mean local efficiency (B), modularity (C) and clustering coefficient (D) (y-axis) over increasing network densities (x-axis), after adjustment for age and gender, for each group. Each hash (#) symbol (aligned to the x-axis) indicates a significant difference at each network density with the color indicating the groups compared. Dark blue (#) indicates significance for HC vs AD. Light blue (#) indicates significance for NPS_NA vs NPS_A. Light green (#) indicates significance for NPS_None vs NPS_A. In those with AD compared to HC, modularity was higher (C) suggesting increased segregation of networks. In NPS_A, local density of connections are lower as suggested by lower local efficiency (B) and clustering coefficient (D) whereas global efficiency in the AD and NPS_A groups are highly similar (A). (For interpretation of the references to color in this figure legend, the reader is referred to the web version of this article.)

efficiency and clustering coefficient were lower than in the NPS_None and NPS_NA groups, suggesting that segregation of neural processing may be affected. Global efficiency was also altered in the NPS_A group, as compared to the NPS_None and NPS_NA groups. Fig. 2A shows that values of global efficiency in the apathy group were similar to the AD

group. Together, these results suggest that apathy may be associated with reduced nodal density of functional connections. The findings from network level analysis in both network definitions converge upon the FPN where participation coefficient was higher while local efficiency was similar in NPS_A compared to the NPS_None and NPS_NA
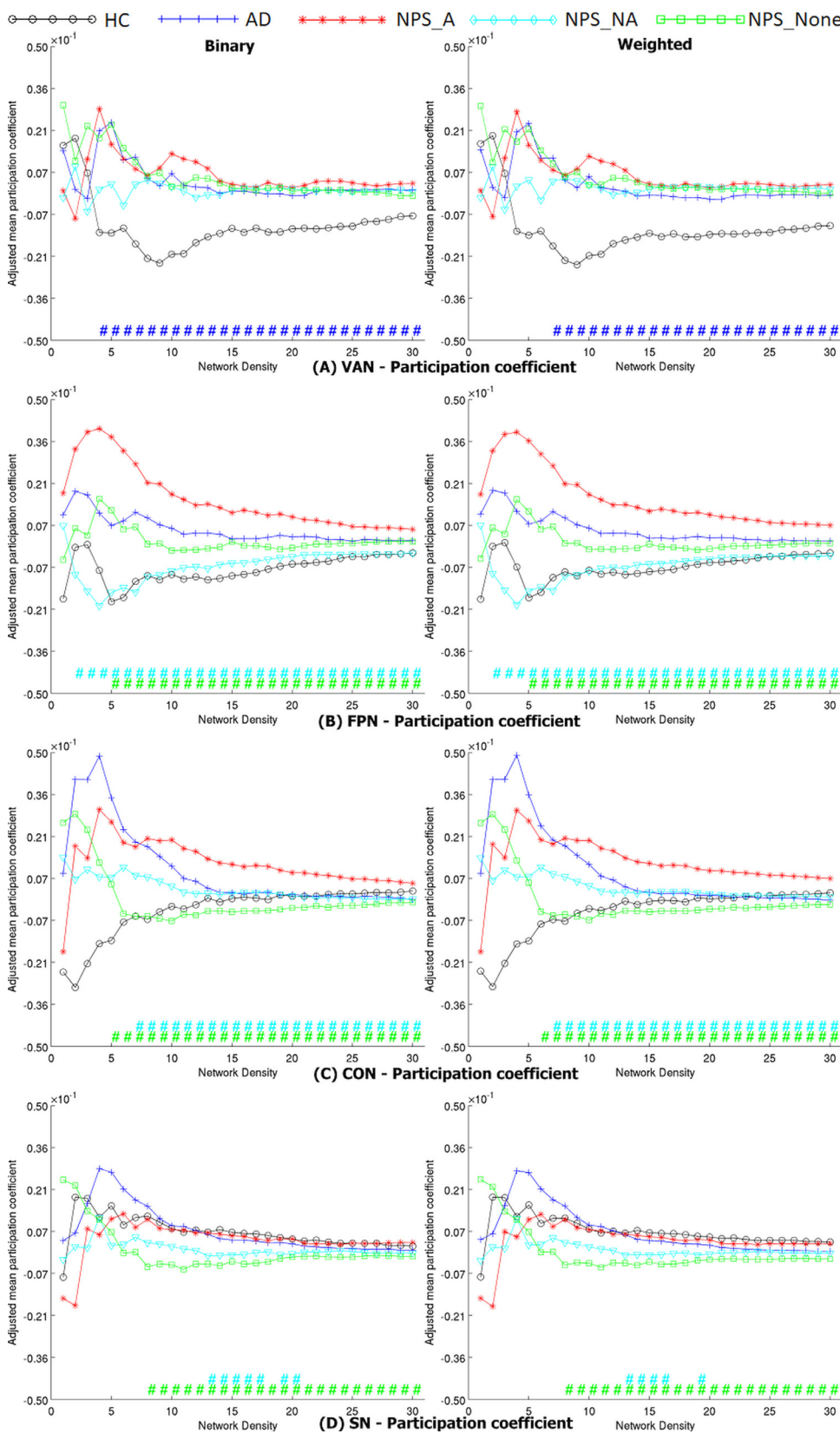
Fig. 3. Graph theoretical properties in current sample networks. The figures show the binary (left) and weighted (right) mean local efficiency (y-axis) in the dACC (A), and mean participation coefficient (y-axis) over increasing network densities (x-axis) in the dACC (B), Insulo-temporoparietal network (C), and frontoparietal network (D), after adjustment for age and gender, for each group. Each hash (#) symbol (aligned to the x-axis) indicates a significant difference at each network density with the color indicating the groups compared. Dark blue (#) indicates significance for HC vs AD. Light blue (#) indicates significance for NPS_NA vs NPS_A. Light green (#) indicates significance for NPS_None vs NPS_A. The NPS_A group shows similar changes as the AD group in local efficiency in dACC (A) and participation coefficient in the insulo-temporoparietal network (C). However, participation coefficient of the dACC (B) in the NPS_A group and AD diverge. Taking (A) and (B) together suggests that inter-network edges in NPS_A are lost to a greater extent than in AD. In contrast, changes in FPN in form of increased participation coefficient may be specific to the NPS_A group. (For interpretation of the references to color in this figure legend, the reader is referred to the web version of this article.)

groups. This suggests that reduced segregation of the FPN is associated with apathy in AD. Similar findings for the CON also suggest reduced segregation of this network in association with apathy. Finally, findings for the dACC were indicative of increased segregation in this network in patients with apathy.

Symptoms of apathy are proposed to arise from deficits in neural circuits linking the frontal cortex to the basal ganglia (Levy and Dubois, 2006). As noted above, apathy in MCI and AD patients was not only associated with fronto-subcortical circuits but also with broader regions of the association cortex (Kos et al., 2016; Stella et al., 2014;
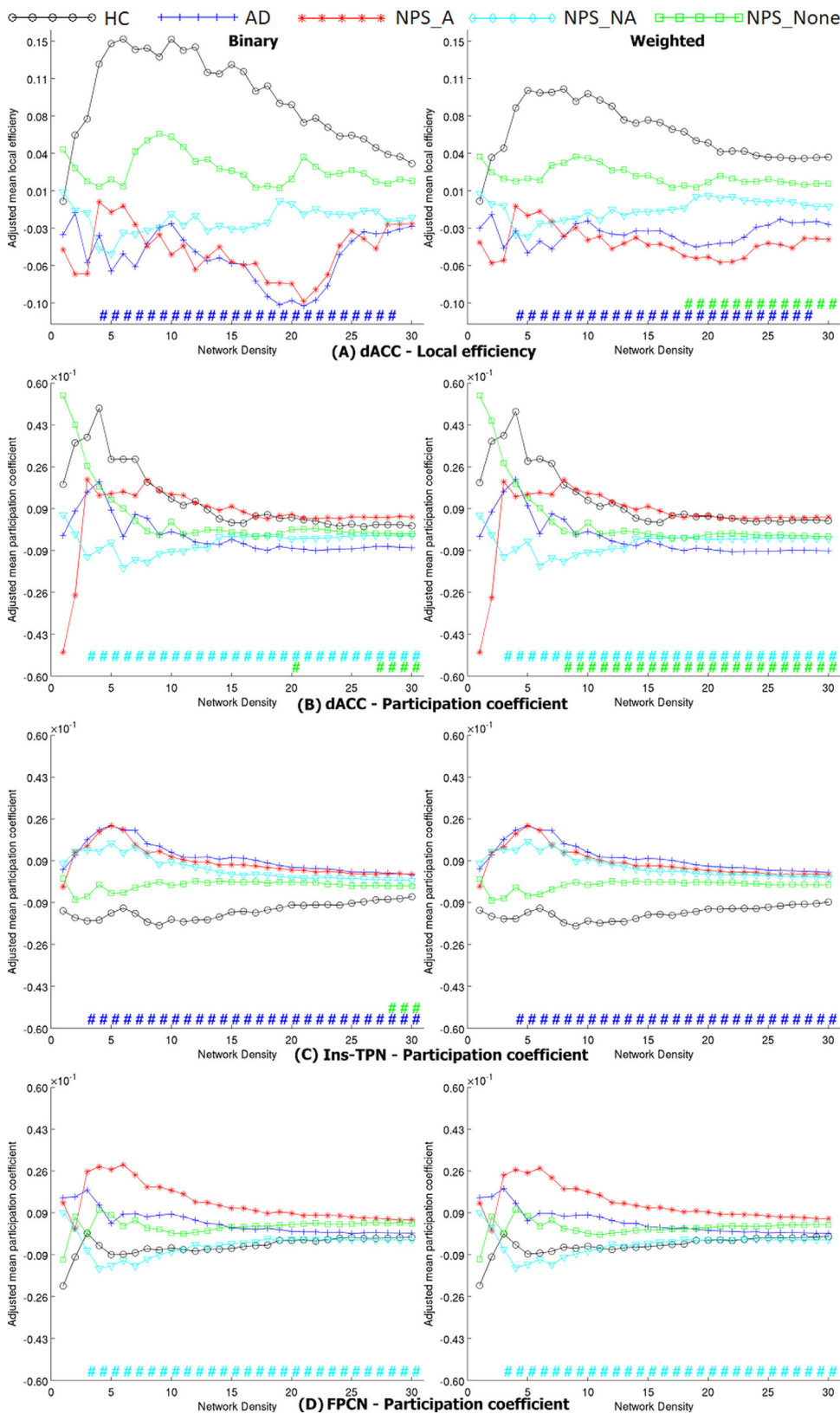
Fig.. 4. Group difference in independently-defined networks. The figures show the binary (left) and weighted (right) mean participation coefficient (y-axis) over increasing network densities (x-axis) in the ventral attention network (A), frontoparietal network (B), cingulo-opercular network (C), and salience network (D), after adjustment for age and gender, for each group. Each hash (#) symbol (aligned to the x-axis) indicates a significant difference at each network density with the color indicating the groups compared. Dark blue (#) indicates significance for HC vs AD. Light blue (#) indicates significance for NPS_NA vs NPS_A. Light green (#) indicates significance for NPS_None vs NPS_A. Increased participation coefficient in the frontoparietal network (B) and cingulo-opercular network (C) was present to a greater extent in the NPS_A group whereas all patient groups show similarly increased participation coefficient in the ventral attention network (A). In the salience network (D), the NPS_None group shows lower participation coefficient, which may indicate compensatory changes that preserve function. (For interpretation of the references to color in this figure legend, the reader is referred to the web version of this article.)

Theleritis et al., 2014). The findings of the present study extend this knowledge, showing that functional connectivity of the FPN and CON is altered in apathy. It is noteworthy that these networks have been implicated in the control of goal-directed action, (Dosenbach et al., 2007) as goal-directed behavior is proposed to be reduced in apathy (Levy and Dubois, 2006; Robert et al., 2009). Each of these networks are

suggested to support distinct aspects of task execution. Whereas the FPN is associated with rapid and adaptive execution of tasks, the CON is associated with the maintenance of sustained attention and stable task-representations (Dosenbach et al., 2007; Sadaghiani et al., 2010; Seeley et al., 2009). Based on the suggested cognitive functions of these networks, the current findings indicate that patients with apathy may

be impaired in encoding as well as executing goal-directed behavior (Tumati et al., 2019). This interpretation is consistent with symptoms of apathy such as needing to be told what to do or difficulty in initiating actions. As both networks were associated with apathy, it may be possible that dysfunction in each network produces symptoms of apathy, forming distinct neural routes.

Recent studies have found that apathy in aMCI patients was associated with reduced connectivity in the FPN (Joo et al., 2017; Moretti et al., 2017; Munro et al., 2015). Results of the current study support this finding, and additionally, functional changes in the CON are consistent with previous studies associating structural, functional, and metabolic changes in the dACC and temporo-parietal lobe with apathy (Kos et al., 2016; Stella et al., 2014; Tumati et al., 2018; Yeh et al., 2018). The current results are also likely to be more robust as compared to previous studies of functional connectivity in apathy due to differences in methodology. First, functional connectivity was assessed in the whole brain, and in a seven as well as ten functional network parcellation providing a fine-grained analysis as opposed to the evaluation of selective ROIs limited to three to four functional networks in past studies (Balthazar et al., 2014; Munro et al., 2015). Second, as NPS are often comorbid especially with increasing severity of AD, (Forrester et al., 2016) associating brain changes to a specific NPS is challenging. In the current study, a novel approach was used: contrasting graph measures in patients with apathy to patients without NPS (NPS_None) and those with NPS other than apathy (NPS_NA). Only significant changes in a graph measure in both comparisons were considered to be specific to apathy. Finally, studies of apathy may be confounded by comorbid depression as the clinical picture of the two symptoms may be similar (Palmer et al., 2010; Starkstein et al., 2005). As subjects with a moderate-to-high depression score at baseline (GDS > 5) were excluded in the parent ADNI study, from which the current sample is drawn, comorbid depression is unlikely to affect the results. Together, these factors improve the specificity of the detected brain changes in association with apathy as compared to past studies.

Besides network-level topological alterations, apathy was also associated with changes in global graph measures. The changes in local efficiency and global efficiency suggest that apathy is associated with reduced global integration whereas the modularity metric indicates that segregation or the overall community structure of networks, is not affected in apathy. The current results also suggest that NPS may be associated with specific topological changes in AD. For example, global efficiency (Fig. 2A) and local efficiency of dACC (Fig. 3A) were highly similar in AD and NPS_A groups. Correspondingly, all patient groups (AD, NPS_A, NPS_None & NPS_NA) showed similar participation coefficient of the ventral attention network (Fig. 4A) and insulo-temporoparietal network (Fig. 3C) whereas participation coefficient of the somatomotor network was lower only in the NPS_None group (SI Fig. 3). Studies of topology indicate that an increase in modularity and path length (reduced efficiency) occur in MCI and AD (Brier et al., 2014; Dai et al., 2015; Deng et al., 2016; Liu et al., 2014). Considering the current results, further investigation of functional brain changes associated with NPS are warranted to determine their role in network dysfunction in AD. Moreover, the disease state (MCI versus AD) may also be associated with specific network dysfunction as indicated by our exploratory findings. Whether such subject characteristics, including gender, are related to network changes in apathy remain a relevant topic for future study.

4.1. Limitations

As noted above, apathy is associated with an increased risk of AD and identifying the neural changes specific to apathy is challenging. Our novel approach of comparing subjects in the NPS_A, NPS_NA, and NPS_None partially addresses this issue. Secondly, because apathy was diagnosed with the NPI, we were unable to investigate its severity and its proposed sub-types that may have distinct neural mechanisms

(Levy and Dubois, 2006). Future studies may investigate if there are multiple routes to apathy in AD. However, the ADNI is a well characterized dataset and the NPI is a widely used measure of apathy, and hence, these results provide the basis for further investigations. Graph theoretical measures are sensitive to methodological procedures, which have been suggested to result in differences between studies (Tijms et al., 2013). In this study for example, NPS_A was associated with higher GE in binary graphs but reduced GE in weighted graphs. Such results highlight the complexity of graph measures and interpreting such findings may be challenging (De Vico Fallani et al., 2014; Kuang et al., 2019). Processing steps such as ignoring negative correlations in building graphs or the use of global signal regression may also affect results. Therefore, replication of findings in an independent sample is essential. Furthermore, the organization of brain networks is affected by variables such as age and disease. By using functional networks defined in a healthy independent sample and in the study sample, we aimed to minimize such effects. Nevertheless, methodological differences in defining the network structures need to be considered.

In summary, the results of the current study in a sample of MCI and AD subjects without comorbid depression suggest that apathy in AD is associated with increased segregation of the frontoparietal network and the cingulo-opercular network. Further, the dACC shows a marked reduction in efficiency and increased segregation in association with apathy. Finally, global changes suggest that localized loss of functional connections may contribute to the development of apathy.

CRediT authorship contribution statement

Shankar Tumati: Conceptualization, Data curation, Formal analysis, Software, Visualization, Writing - original draft, Writing - review & editing. **Jan-Bernard C. Marsman:** Conceptualization, Formal analysis, Software, Validation, Writing - review & editing. **Peter Paul De Deyn:** Methodology, Supervision, Writing - review & editing. **Sander Martens:** Supervision, Writing - review & editing. **André Aleman:** Conceptualization, Resources, Supervision, Writing - review & editing.

Declaration of Competing Interest

The authors have no conflicts of interest to declare.

providing funds to support ADNI clinical sites in Canada. Private sector contributions are facilitated by the Foundation for the National Institutes of Health (www.fnih.org). The grantee organization is the Northern California Institute for Research and Education, and the study is coordinated by the Alzheimer's Disease Cooperative Study at the University of California, San Diego. ADNI data are disseminated by the Laboratory for Neuro Imaging at the University of Southern California. ADNI or the funders did not play any role in the analysis or writing of the present study.

Supplementary materials

Supplementary material associated with this article can be found, in the online version, at doi:10.1016/j.jad.2020.01.158.

References

Balthazar, M.L.F., Pereira, F.R.S., Lopes, T.M., da Silva, E.L., Coan, A.C., Campos, B.M., Duncan, N.W., Stella, F., Northoff, G., Damasceno, B.P., Cendes, F., 2014. Neuropsychiatric symptoms in Alzheimer's disease are related to functional connectivity alterations in the salience network. Hum. Brain Mapp. 35, 1237–1246. https://doi.org/10.1002/hbm.22248.

Brier, M.R., Thomas, J.B., Fagan, A.M., Hassenstab, J., Holtzman, D.M., Benzinger, T.L., Morris, J.C., Ances, B.M., 2014. Functional connectivity and graph theory in preclinical Alzheimer's disease. Neurobiol. Aging 35, 757–768. https://doi.org/10.1016/j.neurobiolaging.2013.10.081.

Bullmore, E., Sporns, O., 2009. Complex brain networks: graph theoretical analysis of structural and functional systems. Nat. Rev. Neurosci. 10, 186–198. https://doi.org/10.1038/nrn2575.

Cummings, J.L., Mega, M., Gray, K., Rosenberg-Thompson, S., Carusi, D.A., Gornbein, J., 1994. The neuropsychiatric inventory: comprehensive assessment of psychopathology in dementia. Neurology 44, 2308–2314. https://doi.org/10.1212/wnl.44.12.2308.

Dai, Z., Yan, C., Li, K., Wang, Z., Wang, J., Cao, M., Lin, Q., Shu, N., Xia, M., Bi, Y., He, Y., 2015. Identifying and mapping connectivity patterns of brain network hubs in Alzheimer's disease. Cereb. 3723–3742. https://doi.org/10.1093/cercor/bhu246. Cortex N. Y. N 1991 25.

De Vico Fallani, F., Richiardi, J., Chavez, M., Achard, S., 2014. Graph analysis of functional brain networks: practical issues in translational neuroscience. Philos. Trans. R. Soc. Lond. B. Biol. Sci. 369. https://doi.org/10.1098/rstb.2013.0521.

Deng, Y., Liu, K., Shi, L., Lei, Y., Liang, P., Li, K., Chu, W.C.W., Wang, D., Alzheimer's Disease Neuroimaging Initiative, 2016. Identifying the alteration patterns of brain functional connectivity in progressive mild cognitive impairment patients: a longitudinal whole-brain voxel-wise degree analysis. Front. Aging Neurosci. 8, 195. https://doi.org/10.3389/fnagi.2016.00195.

Dosenbach, N.U.F., Fair, D.A., Miezin, F.M., Cohen, A.L., Wenger, K.K., Dosenbach, R.A.T., Fox, M.D., Snyder, A.Z., Vincent, J.L., Raichle, M.E., Schlaggar, B.L., Petersen, S.E., 2007. Distinct brain networks for adaptive and stable task control in humans. Proc. Natl. Acad. Sci. U. S. A. 104, 11073–11078. https://doi.org/10.1073/pnas.0704320104.

Filippi, M., Basaia, S., Canu, E., Imperiale, F., Magnani, G., Falautano, M., Comi, G., Falini, A., Agosta, F., 2018. Changes in functional and structural brain connectome along the Alzheimer's disease continuum. Mol. Psychiatry. https://doi.org/10.1038/s41380-018-0067-8.

Forrester, S.N., Gallo, J.J., Smith, G.S., Leoutsakos, J.-M.S., 2016. Patterns of neuropsychiatric symptoms in mild cognitive impairment and risk of dementia. Am. J. Geriatr. Psychiatry Off. J. Am. Assoc. Geriatr. Psychiatry 24, 117–125. https://doi.org/10.1016/j.jagp.2015.05.007.

Geda, Y.E., Roberts, R.O., Knopman, D.S., Petersen, R.C., Christianson, T.J.H., Pankratz, V.S., Smith, G.E., Boeve, B.F., Ivnik, R.J., Tangalos, E.G., Rocca, W.A., 2008. Prevalence of neuropsychiatric symptoms in mild cognitive impairment and normal cognitive aging: population-based study. Arch. Gen. Psychiatry 65, 1193–1198. https://doi.org/10.1001/archpsyc.65.10.1193.

Joo, S.H., Lee, C.U., Lim, H.K., 2017. Apathy and intrinsic functional connectivity networks in amnestic mild cognitive impairment. Neuropsychiatr. Dis. Treat. 13, 61–67. https://doi.org/10.2147/NDT.S123338.

Kos, C., van Tol, M.-J., Marsman, J.-B.C., Knegtering, H., Aleman, A., 2016. Neural correlates of apathy in patients with neurodegenerative disorders, acquired brain injury, and psychiatric disorders. Neurosci. Biobehav. Rev. 69, 381–401. https://doi.org/10.1016/j.neubiorev.2016.08.012.

Kuang, L., Han, X., Chen, K., Caselli, R.J., Reiman, E.M., Wang, Y., Alzheimer's Disease Neuroimaging Initiative, 2019. A concise and persistent feature to study brain resting-state network dynamics: findings from the Alzheimer's disease neuroimaging initiative. Hum. Brain Mapp. 40, 1062–1081. https://doi.org/10.1002/hbm.24383.

Landau, S.M., Mintun, M.A., Joshi, A.D., Koeppe, R.A., Petersen, R.C., Aisen, P.S., Weiner, M.W., Jagust, W.J., Alzheimer's Disease Neuroimaging Initiative, 2012. Amyloid deposition, hypometabolism, and longitudinal cognitive decline. Ann. Neurol. 72, 578–586. https://doi.org/10.1002/ana.23650.

Levy, R., Dubois, B., 2006. Apathy and the functional anatomy of the prefrontal cortex-basal ganglia circuits. Cereb. 916–928. https://doi.org/10.1093/cercor/bhj043. Cortex N. Y. N 1991 16.

Liu, Y., Yu, C., Zhang, X., Liu, J., Duan, Y., Alexander-Bloch, A.F., Liu, B., Jiang, T., Bullmore, E., 2014. Impaired long distance functional connectivity and weighted network architecture in Alzheimer's disease. Cereb. 1422–1435. https://doi.org/10.1093/cercor/bhs410. Cortex N. Y. N 1991 24.

Moretti, R., Caberlotto, R., Signori, R., 2017. Apathy in corticobasal degeneration: possible parietal involvement. Funct. Neurol. 22, 201–210.

Munro, C.E., Donovan, N.J., Guercio, B.J., Wigman, S.E., Schultz, A.P., Amariglio, R.E., Rentz, D.M., Johnson, K.A., Sperling, R.A., Marshall, G.A., 2015. Neuropsychiatric symptoms and functional connectivity in mild cognitive impairment. J. Alzheimers Dis. JAD 46, 727–735. https://doi.org/10.3233/JAD-150017.

Nobis, L., Husain, M., 2018. Apathy in Alzheimer's disease. Curr. Opin. Behav. Sci., Apathy Motiv. 22, 7–13. https://doi.org/10.1016/j.cobeha.2017.12.007.

Onyike, C.U., Sheppard, J.-M.E., Tschanz, J.T., Norton, M.C., Green, R.C., Steinberg, M., Welsh-Bohmer, K.A., Breitner, J.C., Lyketsos, C.G., 2007. Epidemiology of apathy in older adults: the cache county study. Am. J. Geriatr. Psychiatry Off. J. Am. Assoc. Geriatr. Psychiatry 15, 365–375. https://doi.org/10.1097/01.JGP.0000235689.42910.0d.

Palmer, K., Di Iulio, F., Varsi, A.E., Gianni, W., Sancesario, G., Caltagirone, .C.., Spalletta, G., 2010. Neuropsychiatric predictors of progression from amnestic-mild cognitive impairment to Alzheimer's disease: the role of depression and apathy. J. Alzheimers Dis. JAD 20, 175–183. https://doi.org/10.3233/JAD-2010-1352.

Pereira, J.B., Mijalkov, M., Kakaei, E., Mecocci, P., Vellas, B., Tsolaki, M., Kłoszewska, I., Soininen, H., Spenger, C., Lovestone, S., Simmons, A., Wahlund, L.-O., Volpe, G., Westman, E., AddNeuroMed consortium, 2016. For the Alzheimer's disease neuroimaging initiative. Disrupted Netw. Topol. Patients Stable Prog. Mild Cogn. Imp. Alzheimer's Dis. 26, 3476–3493. https://doi.org/10.1093/cercor/bhw128. Cereb. Cortex N. Y. N 1991.

Pfeffer, R.I., Kurosaki, T.T., Harrah, C.H., Chance, J.M., Filos, S., 1982. Measurement of functional activities in older adults in the community. J. Gerontol. 37, 323–329. https://doi.org/10.1093/geronj/37.3.323.

Power, J.D., Cohen, A.L., Nelson, S.M., Wig, G.S., Barnes, K.A., Church, J.A., Vogel, A.C., Laumann, T.O., Miezin, F.M., Schlaggar, B.L., Petersen, S.E., 2011. Functional network organization of the human brain. Neuron 72, 665–678. https://doi.org/10.1016/j.neuron.2011.09.006.

Power, J.D., Mitra, A., Laumann, T.O., Snyder, A.Z., Schlaggar, B.L., Petersen, S.E., 2014. Methods to detect, characterize, and remove motion artifact in resting state fMRI. Neuroimage 84, 320–341. https://doi.org/10.1016/j.neuroimage.2013.08.048.

Robert, P., Onyike, C.U., Leentjens, A.F.G., Dujardin, K., Aalten, P., Starkstein, S., Verhey, F.R.J., Yessavage, J., Clement, J.P., Drapier, D., Bayle, F., Benoit, M., Boyer, P., Lorca, P.M., Thibaut, F., Gauthier, S., Grossberg, G., Vellas, B., Byrne, J., 2009. Proposed diagnostic criteria for apathy in Alzheimer's disease and other neuropsychiatric disorders. Eur. Psychiatry J. Assoc. Eur. Psychiatr. 24, 98–104. https://doi.org/10.1016/j.eurpsy.2008.09.001.

Rubinov, M., Sporns, O., 2010. Complex network measures of brain connectivity: uses and interpretations. Neuroimage 52, 1059–1069. https://doi.org/10.1016/j.neuroimage.2009.10.003.

Sadaghiani, S., Scheeringa, R., Lehongre, K., Morillon, B., Giraud, A.-.L., Kleinschmidt, A., 2010. Intrinsic connectivity networks, alpha oscillations, and tonic alertness: a simultaneous electroencephalography/functional magnetic resonance imaging study. J. Neurosci. Off. J. Soc. Neurosci. 30, 10243–10250. https://doi.org/10.1523/JNEUROSCI.1004-10.2010.

Seeley, W.W., Crawford, R.K., Zhou, J., Miller, B.L., Greicius, M.D., 2009. Neurodegenerative diseases target large-scale human brain networks. Neuron 62, 42–52. https://doi.org/10.1016/j.neuron.2009.03.024.

Smith, S.M., Nichols, T.E., 2009. Threshold-free cluster enhancement: addressing problems of smoothing, threshold dependence and localisation in cluster inference. Neuroimage 44, 83–98. https://doi.org/10.1016/j.neuroimage.2008.03.061.

Spalletta, G., Musicco, M., Padovani, A., Rozzini, L., Perri, R., Fadda, L., Canonico, V., Trequattrini, A., Pettenati, C., Caltagirone, C., Palmer, K., 2010. Neuropsychiatric symptoms and syndromes in a large cohort of newly diagnosed, untreated patients with Alzheimer disease. Am. J. Geriatr. Psychiatry Off. J. Am. Assoc. Geriatr. Psychiatry 18, 1026–1035. https://doi.org/10.1097/JGP.0b013e3181d6b68d.

Starkstein, S.E., Brockman, S., 2018. The neuroimaging basis of apathy: empirical findings and conceptual challenges. Neuropsychologia. https://doi.org/10.1016/j.neuropsychologia.2018.01.042.

Starkstein, S.E., Ingram, L., Garau, M.L., Mizrahi, R., 2005. On the overlap between apathy and depression in dementia. J. Neurol. Neurosurg. Psychiatry 76, 1070–1074. https://doi.org/10.1136/jnnp.2004.052795.

Stella, F., Radanovic, M., Aprahamian, I., Canineu, P.R., de Andrade, L.P., Forlenza, O.V., 2014. Neurobiological correlates of apathy in Alzheimer's disease and mild cognitive impairment: a critical review. J. Alzheimers Dis. JAD 39, 633–648. https://doi.org/10.3233/JAD-131385.

Theleritis, C., Politis, A., Siarkos, K., Lyketsos, C.G., 2014. A review of neuroimaging findings of apathy in Alzheimer's disease. Int. Psychogeriatr. IPA 26, 195–207. https://doi.org/10.1017/S1041610213001725.

Tijms, B.M., Wink, A.M., de Haan, W., van der Flier, W.M., Stam, C.J., Scheltens, P., Barkhof, F., 2013. Alzheimer's disease: connecting findings from graph theoretical studies of brain networks. Neurobiol. Aging 34, 2023–2036. https://doi.org/10.1016/j.neurobiolaging.2013.02.020.

Tumati, S., Martens, S., de Jong, B.M., Aleman, A., 2019. Lateral parietal cortex in the generation of behavior: implications for apathy. Prog. Neurobiol. 175, 20–34. https://doi.org/10.1016/j.pneurobio.2018.12.003.

Tumati, S., Opmeer, E.M., Marsman, J.-B.C., Martens, S., Reesink, F.E., De Deyn, P.P., Aleman, A., 2018. Lower choline and myo-inositol in temporo-parietal cortex is associated with apathy in amnestic mci. Front. Aging Neurosci. 10, 106. https://doi.org/10.3389/fnagi.2018.00106.

Van Dijk, K.R.A., Sabuncu, M.R., Buckner, R.L., 2012. The influence of head motion on intrinsic functional connectivity MRI. Neuroimage 59, 431–438. https://doi.org/10.1016/j.neuroimage.2011.07.044.

Yeh, Y.-C., Li, C.-W., Kuo, Y.-T., Huang, M.-F., Liu, T.-L., Jaw, T.-S., Yang, Y.-H., Kuo, K.-C., Chen, C.-S., 2018. Association between altered neurochemical metabolites and apathy in patients with Alzheimer's disease. Int. Psychogeriatr. 30, 761–768. https://doi.org/10.1017/S1041610217002381.